

Hydrogen Generation by Hangman Metalloporphyrins

Chang Hoon Lee, Dilek K. Dogutan, and Daniel G. Nocera*

Department of Chemistry, 6-335, Massachusetts Institute of Technology, 77 Massachusetts Avenue, Cambridge, Massachusetts 02139-4307, United States

S Supporting Information

ABSTRACT: A cobalt(II) hangman porphyrin with a xanthen backbone and a carboxylic acid hanging group catalyzes the electrochemical production of hydrogen from benzoic and tosic acid in acetonitrile solutions. We show that $\text{Co}^{\text{II}}\text{H}$ is exclusively involved in the generation of H_2 from weak acids. In a stronger acid, a $\text{Co}^{\text{III}}\text{H}$ species is observed electrochemically, but it still needs to be further reduced to $\text{Co}^{\text{II}}\text{H}$ before H_2 generation occurs. Overpotentials for H_2 generation are lowered as a result of the hangman effect.

Hydrogen generation from carbon-neutral sources is an important part of a multifaceted strategy to meet growing global energy demands.^{1,2} Accordingly, renewed interest in H_2 catalyst discovery has led to the creation of a variety of complexes that electrocatalyze H^+ reduction.^{3–9} A particularly fascinating design element of emergent catalysts is the incorporation of a proton relay from a pendant acid–base group proximate to the metal center where H_2 production occurs.^{3,4,10,11} These catalysts are akin to the active sites of hydrogenases, which feature pendant bases positioned near the metal centers that are postulated to play a role in enzyme catalysis.¹² The benefits of a pendant proton relay are consistent with the early proposal of H_2 generation via the pathway shown in Scheme 1A: reduction of a Co^{II} center to Co^{I} followed by H^+ attack to yield a hydridic $\text{Co}^{\text{III}}\text{H}$ species that yields H_2 upon protonolysis or bimetallic reaction. However, this mechanism has been recently reconsidered in view of the contention that $\text{Co}^{\text{III}}\text{H}$ centers are not sufficiently basic to drive protonolysis, and it has been suggested that more reduced cobalt species must be attained before protonolysis can occur (Scheme 1B).^{13,14} The inability to control proton stoichiometry in most catalytic cycles has made it difficult to distinguish mechanisms and thus discern which intermediate is involved in catalysis. On this count, we realized the utility of hangman active sites for providing insight into the mechanism of H_2 evolution by stoichiometric generation of a key intermediate as a result of the hangman effect. In the hangman construction, an acid–base functionality is positioned from a xanthen or furan spacer over the face of a redox-active macrocycle such as porphyrin,^{15,16} salen,^{17,18} or corrole.¹⁹ The acid–base hanging group permits the facile transfer of a single proton to or from a substrate bound to a metal macrocycle. With the ability to control proton stoichiometry from the hanging group, we undertook studies to examine H_2 generation at $\text{CoHPX-CO}_2\text{H}$ (**1-Co**), shown in Chart 1. Comparison of the electrochemistry of **1-Co** to that of a macrocyclic analogue in which the hanging group has been removed, CoHPX-Br (**2-Co**, Chart 1), establishes the

Scheme 1

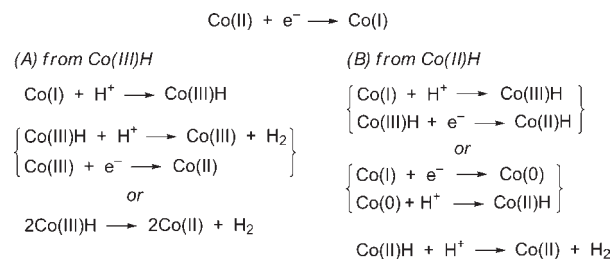
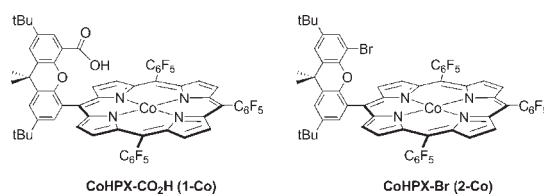


Chart 1



hangman effect (via a reduced overpotential) and that the Co^{I} center produces H_2 beyond reduction potentials exceeding the Co^{I} oxidation state. Our results are consistent with the generation of $\text{Co}^{\text{II}}\text{H}$ as a key intermediate in H_2 electrocatalysis at the hangman cobalt porphyrin active sites.

Hangman porphyrins can be obtained in appreciable quantities, in short synthesis times, and in high yields.^{20,21} **1-Co** and **2-Co** were synthesized following these methods. As shown in Figure 1a, **1-Co** and **2-Co** exhibit reversible waves for the $\text{Co}^{\text{II/I}}$ couple at almost the same potentials (-1.08 V vs the ferrocene/ferrocenium couple for **1-Co** and -1.10 V for **2-Co**). The cyclic voltammogram (CV) of **2-Zn** shows redox waves at -1.52 and -1.92 V (Supporting Information (SI) Figure S9) and confirms that each electrochemical feature of **1-Co** and **2-Co** has significant cobalt character. For simplicity, the reduction potentials will be formally ascribed to Co , though we believe that there is significant electron density on the porphyrin ring at very reducing potentials.

Whereas **2-Co** shows a reversible wave for $\text{Co}^{\text{I/0}}$ at -2.14 V, interestingly, **1-Co** produces an irreversible wave for the reduction of Co^{I} , and the wave is positively shifted by ~ 200 mV. The only structural difference between **1-Co** and **2-Co** is the hanging carboxylic acid group, and accordingly the irreversible process of

Received: March 8, 2011

Published: May 10, 2011

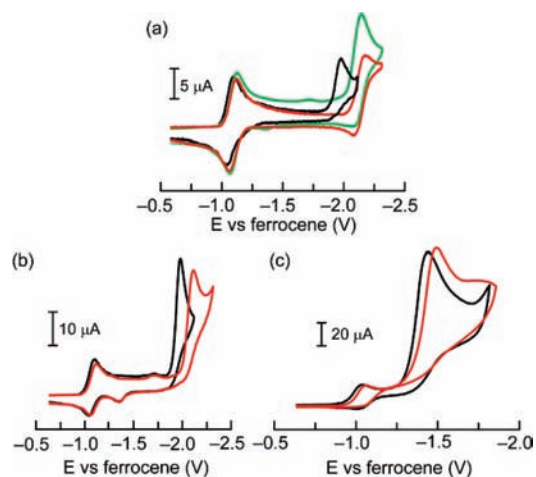


Figure 1. (a) CVs of 0.5 mM **1-Co** (black line), **2-Co** (red line), and **2-Co** in the presence of 0.5 mM benzoic acid (green line). (b) CVs of 0.5 mM **1-Co** in the presence of 2.5 mM benzoic acid (black line) and 0.5 mM **2-Co** in the presence of 3.0 mM benzoic acid (red line). (c) CVs of 0.8 mM **1-Co** (black line) and **2-Co** (red line) in the presence of 10 mM tosic acid. Scan rate, 100 mV/s; 0.1 M NBu_4PF_6 in acetonitrile. Glassy carbon working electrode, Ag/AgNO_3 reference electrode, and Pt wire counter electrode.

1-Co is ascribed to the hangman effect, where the reduction of Co^{I} to Co^{0} is followed by immediate proton transfer from the hanging group to produce $\text{Co}^{\text{II}}\text{H}$. The second wave in the CV of **2-Co** also becomes irreversible upon the addition of external benzoic acid. At 1 equiv of benzoic acid, the wave begins to exhibit irreversibility, also indicating protonation of the Co^{0} species. Complete irreversibility of the wave is observed only upon addition of >1 equiv of benzoic acid; this observation is consistent with the hangman effect in **1-Co**.

In the presence of excess benzoic acid ($\text{p}K_{\text{a}} = 20.7$ in acetonitrile),²² **1-Co** and **2-Co** exhibit catalytic cathodic waves (Figure 1b and SI Figures S2 and S3). Whereas the overpotential for catalysis is large (~ 800 mV), the catalysis performance is not our interest; the CV features of the electrocatalysis uncover essential mechanistic details of the hydrogen evolution reaction (HER) at cobalt macrocycles. The $\text{Co}^{\text{II}/\text{I}}$ reduction feature is not affected much by the presence of acid (SI Figures S2, S3, and S8), but the second reduction wave exhibits pronounced catalytic activity. These results indicate that benzoic acid is too weak an acid to protonate the Co^{I} center, and hence catalytic H_2 production is observed only upon further reduction to Co^{0} . The overpotential for proton reduction of **1-Co** is ~ 120 mV lower than that of **2-Co** at 3 mM acid concentration. Moreover, the potential of the second reduction wave of **1-Co** is the same in the presence and absence of acid (Figure S2). This is not the case for **2-Co**; with increasing acid concentration, the wave shifts to more positive potential by 80 mV (Figure S3). These results are also indicative of the hangman effect since in **1-Co**, proton transfer is not rate-determining for catalysis (hence the insensitivity of the reduction wave to proton concentration), whereas in **2-Co**, the proton transfer is a determinant of the mechanism (hence the shift to more positive potential with increasing acid). For either case, H_2 catalysis is initiated from the $\text{Co}^{\text{II}}\text{H}$.

Bulk electrolysis was performed in acetonitrile solutions of 0.4 mM **1-Co** at -2.05 V and of 0.5 mM **2-Co** at -2.20 V in the presence of 15 mM benzoic acid. The amount of H_2 gas produced

during the electrolysis was determined by gas chromatography after 15 C of charges had passed. Faradaic efficiencies for H_2 production were ca. 80% and 85% for **1-Co** and **2-Co**, respectively; no other gaseous product is detected in the experimental condition. On the basis of TLC, mass spectra, and UV–vis measurements, the decomposed product in bulk electrolysis in the presence of **2-Co** does not correspond to a demetalated porphyrin or other porphyrin product.

In the presence of the stronger tosic acid ($\text{p}K_{\text{a}} = 8.3$ in acetonitrile²²), both **1-Co** and **2-Co** exhibit catalytic cathodic waves at ~ -1.5 V (Figures 1c and SI Figures S4 and S5). The similarity of the CVs with regard to current and the onset of electrocatalysis suggests that the stronger acid overwhelms the chemistry of the system and the hangman effect is obviated. As observed for benzoic acid, electrocatalysis for **1-Co** and **2-Co** occurs at potentials negative of the $\text{Co}^{\text{II}/\text{I}}$ couple. However, there is one significant difference between the benzoic acid and tosic acid data: unlike the situation for benzoic acid, the $\text{Co}^{\text{II}/\text{I}}$ wave becomes irreversible in the stronger tosic acid for both **1-Co** and **2-Co** (Figures 1c, S4, and S5). This indicates that Co^{I} is protonated by the tosic acid. But the observation that catalysis occurs well past the $\text{Co}^{\text{II}/\text{I}}$ reduction event indicates that a $\text{Co}^{\text{III}}\text{H}$ species, when formed, needs to be further reduced to $\text{Co}^{\text{II}}\text{H}$ for H_2 generation to occur. One determinant of the metal basicity is the presence of meso groups on the macrocycle periphery. The electron-withdrawing C_6F_5 groups will attenuate the metal center basicity and make the metal less reactive to protons, as has previously been observed.^{6,23}

In summary, the hangman porphyrin provides mechanistic insight into H^+ reduction owing to the ability to control proton equivalency precisely via the hanging group. The irreversibility and positive shift of the reduction of Co^{I} in **1-Co** together with a lowered overpotential for H_2 production are results of the hangman effect. For the case of weak acids, H_2 is produced upon reduction to Co^{0} , followed by protonation (middle bracket, Scheme 1B). For stronger acids, Co^{I} is first protonated, and electron reduction follows it (top bracket, Scheme 1B). Regardless of the strength of the acid, these results are consistent with H_2 production being mediated by $\text{Co}^{\text{II}}\text{H}$. Further reduction of the metal is needed for the effective protonation of the hydride to produce H_2 .

■ ASSOCIATED CONTENT

S Supporting Information. Full synthetic details and characterization for **2**, **2-Co**, and **2-Zn**; CVs of **1-Co** and **2-Co** in the presence of benzoic and tosic acid; CVs of benzoic acid and tosic acid; and CV of **2-Zn**. This material is available free of charge via the Internet at <http://pubs.acs.org>.

■ AUTHOR INFORMATION

Corresponding Author
nocera@mit.edu

■ ACKNOWLEDGMENT

We thank the Office of Basic Energy Sciences of the DOE (DE-FG02-05ER15745) for support of this work. Grants from the NSF also provided instrument support to the DCIF at MIT (CHE-9808061, DBI-9729592). We thank Yogesh Surendranath and Kwabena Bediako for helpful discussions.

■ REFERENCES

- (1) Cook, T. R.; Dogutan, D. K.; Reece, S. Y.; Surendranath, Y.; Teets, T. S.; Nocera, D. G. *Chem. Rev.* **2010**, *110*, 6474–6502.
- (2) Lewis, N. S.; Nocera, D. G. *Proc. Natl. Acad. Sci. U.S.A.* **2006**, *103*, 15729–15735.
- (3) Wilson, A. D.; Newell, R. H.; McNevin, M. J.; Muckerman, J. T.; Dubois, M. R.; Dubois, D. L. *J. Am. Chem. Soc.* **2006**, *128*, 358–366.
- (4) Wilson, A. D.; Shoemaker, R. K.; Miedaner, A.; Muckerman, J. T.; Dubois, D. L.; Dubois, M. R. *Proc. Natl. Acad. Sci. U.S.A.* **2007**, *104*, 6951–6956.
- (5) Bigi, J. P.; Hana, T. E.; Harman, W. H.; Chang, A.; Chang, C. J. *Chem. Commun.* **2010**, 958–960.
- (6) Hu, X. L.; Brunschwig, B. S.; Peters, J. C. *J. Am. Chem. Soc.* **2007**, *129*, 8988–8998.
- (7) Baffert, C.; Artero, V.; Fontecave, M. *Inorg. Chem.* **2007**, *46*, 1817–1824.
- (8) Jacques, P.-A.; Artero, V.; Pécaut, J.; Fontecave, M. *Proc. Natl. Acad. Sci. U.S.A.* **2009**, *106*, 20627–20632.
- (9) Grass, V.; Lexa, D.; Saveant, J.-M. *J. Am. Chem. Soc.* **1997**, *119*, 7526–7532.
- (10) Henry, R. M.; Shoemaker, R. K.; DuBois, D. L.; DuBois, M. R. *J. Am. Chem. Soc.* **2006**, *128*, 3002–3010.
- (11) Barton, B. E.; Rauchfuss, T. B. *J. Am. Chem. Soc.* **2010**, *132*, 14877–14885.
- (12) Nicolet, Y.; de Lacey, A. L.; Vèrnedé, X.; Fernandez, V. M.; Hatchikian, E. C.; Fontecilla-Camps, J. C. *J. Am. Chem. Soc.* **2001**, *123*, 1596–1601.
- (13) McCormic, T. M.; Calitree, B. D.; Orchard, A.; Kraut, N. D.; Bright, F. V.; Detty, M. R.; Eisenberg, R. *J. Am. Chem. Soc.* **2010**, *132*, 15480–15483.
- (14) Dempsey, J. L.; Winkler, J. R.; Gray, H. B. *J. Am. Chem. Soc.* **2010**, *132*, 16774–16776.
- (15) Rosenthal, J.; Nocera, D. G. *Prog. Inorg. Chem.* **2007**, *55*, 483–544.
- (16) Rosenthal, J.; Nocera, D. G. *Acc. Chem. Res.* **2007**, *40*, 543–553.
- (17) Liu, S.-Y.; Nocera, D. G. *J. Am. Chem. Soc.* **2005**, *127*, 5278–5279.
- (18) Yang, J. Y.; Nocera, D. G. *J. Am. Chem. Soc.* **2007**, *129*, 8192–8198.
- (19) Dogutan, D. K.; Stoian, S. A.; McGuire, R., Jr.; Schwalbe, M.; Teets, T. S.; Nocera, D. G. *J. Am. Chem. Soc.* **2011**, *133*, 131–140.
- (20) Dogutan, D. K.; Bediako, D. K.; Teets, T. S.; Schwalbe, M.; Nocera, D. G. *Org. Lett.* **2010**, *12*, 1036–1039.
- (21) McGuire, R., Jr.; Dogutan, D. K.; Teets, T. S.; Suntivich, J.; Shao-Horn, Y.; Nocera, D. G. *Chem. Sci.* **2010**, *1*, 411–414.
- (22) Fourmond, V.; Jacques, P.-A. J.; Fontecave, M.; Artero, V. *Inorg. Chem.* **2010**, *49*, 10338–10347.
- (23) Collman, J. P.; Ha, Y.; Wagenknecht, P. S.; Lopez, M. A.; Guilard, R. *J. Am. Chem. Soc.* **1993**, *115*, 9080–9088.